



Original article

Sus Scrofa immune tissues as a new source of bioactive substances for skin wound healing



Alexandr Basov^{a,b}, Liliya Fedulova^c, Ekaterina Vasilevskaya^c, Ekaterina Trofimova^d, Nataliya Murashova^d, Stepan Dzhimak^{b,c,*}

^a Kuban State Medical University, Mitrophana Sedina Street, Krasnodar 350063, Russian Federation

^b Kuban State University, Stavropolskaya Street, 149, Krasnodar 350040, Russian Federation

^c The V.M. Gorbatov Federal Research Center for Food Systems of Russian Academy of Sciences, Talalikhina Street, 26, Moscow 109316, Russian Federation

^d Mendeleev University of Chemical Technology of Russia, Miuskaya Square, 9, Moscow 125047, Russian Federation

ARTICLE INFO

Article history:

Received 9 October 2020

Revised 9 December 2020

Accepted 14 December 2020

Available online 21 December 2020

Keywords:

Protein-peptide complex

BALB/c mice

Skin regeneration

Wound healing

ABSTRACT

Influence of a new protein-peptide complex on promoting skin wound healing in male *BALB/c* mice was studied. Protein-peptide complex, extracted from *Sus scrofa* immune organs, was percutaneously administered using two methods: by lecithin gel-like liquid crystals and by liquid microemulsion. On the fifth day, wound closure in mice with a linear wound model become faster in group (less 2 days comparison to other ones), which was treated with lecithin liquid crystals carrying the protein-peptide complex. This promoting healing can be caused by resorption of bioactive high-molecular compounds the animal skin. In mice with the linear wound model, the tensile strength of the scars were respectively higher both in mice, treated using lecithin liquid crystals with protein-peptide complex, and in mice, treated using microemulsion containing protein-peptide complex, by 215.4% and 161.5% relative to the animals, which did not receive bioactive substances for wound treatment. It was associated with the regenerative effects of tissue- and species-specific protein-peptide complexes, including α -thymosin *Sus scrofa* (C3VVV8_PIG, *m/z* 3802.8) and other factors, which were described as parts of the new extracted complex. This reveals that percutaneous administration of the complex reliably activates local regenerative processes in animals.

© 2020 The Author(s). Published by Elsevier B.V. on behalf of King Saud University. This is an open access article under the CC BY-NC-ND license (<http://creativecommons.org/licenses/by-nc-nd/4.0/>).

1. Introduction

In animals skin damage occurs very often for some reasons, which including acute trauma, chronic wounds, and also consequence of veterinary surgery treatment. It is noteworthy, that technology of using an animal tissues as source of bioactive proteins and peptides is a new trend in veterinary sciences (Baradaran et al., 2017). Biofactors derived from animal tissues, where the main active ingredients are endogenous protein compounds, have

been used to stimulate immunity, metabolic processes, regeneration processes and other (Chen et al., 2019; Crosby and Kronenberg, 2018; Novoseletskaya et al., 2015a, 2015b; Vasilevskaya and Akhremko, 2019). Natural proteins and peptides exhibit higher specificity and effectiveness in comparison to traditional drugs (Kalkhof et al., 2014; Yang et al., 2019).

Earlier, we obtained a complex of tissue-specific proteins from *Sus Scrofa* tissues (Fedulova et al., 2017), which provides the body's primary defense response (Fedulova et al., 2019). Also, these proteins can participate in the secondary immune response and ensure the implementation of regeneration processes. Earlier it was proved that deuterium depleted water (50 ppm) as a solubilizing agent increases the amount of bioactive proteins during extraction (Chernukha et al., 2017). The regulatory effect of this complex has been demonstrated *in vivo* in an immunosuppressed animal model (Fedulova et al., 2017). At the same time, it seems promising to study anti-inflammatory and, in particular decongestant, properties of these native bioactive protein factors with local injuries and systemic pathologies in animals and humans.

* Corresponding author at: Kuban State University, Stavropolskaya Street, 149, Krasnodar 350040, Russian Federation.

E-mail addresses: son_sunytch79@mail.ru (A. Basov), rina715@yandex.ru (L. Fedulova), rina715@yandex.ru (E. Vasilevskaya), namur_home@mail.ru (E. Trofimova), namur_home@mail.ru (N. Murashova), jimack@mail.ru (S. Dzhimak).
Peer review under responsibility of King Saud University.



Production and hosting by Elsevier

<https://doi.org/10.1016/j.sjbs.2020.12.028>

1319-562X/© 2020 The Author(s). Published by Elsevier B.V. on behalf of King Saud University.

This is an open access article under the CC BY-NC-ND license (<http://creativecommons.org/licenses/by-nc-nd/4.0/>).

Traditionally, research of the therapeutic effects of complex protein-based drugs is carried out on animals with various diseases, and using predominantly oral administration (Basov et al., 2019; Chernukha et al., 2018; Fedulova et al., 2018; Gudyrev et al., 2018; Tverskoi et al., 2018). At the same time, percutaneous administration is a highly-promising method of drug administration, because skin is the most extensive and easily accessible organ. Substances applied percutaneously do not mostly pass through the liver; this increases the bioavailability of active components and prolongs systemic exposure (Abdulbaqi et al., 2016). However, the stratum corneum is a highly stable barrier to drug penetration, limiting the transdermal bioavailability of drugs, and therefore special carriers are needed to deliver drug molecules with different physicochemical properties. Due to the use of various delivery systems, molecular protein factors, which are initiating regeneration processes on the mechanical damage model, can penetrate into the target tissues and accumulate there. Damaged skin provides a model for researching the local effects of percutaneous drugs (Chaulagain et al., 2018; Grebennikova and Maklyakov, 2018).

Self-organizing nanostructures of lecithin, such as reverse microemulsions and lyotropic liquid crystals are promising materials for percutaneous drug delivery. They form spontaneously when the necessary components are mixed, and can exist indefinitely at a constant composition and temperature, they are easy to prepare. Lecithin liquid crystals have a higher viscosity and provide a lower rate of release of water-soluble substances, than lecithin microemulsions (Murashova et al., 2019).

So, the aim of this study was to assess the effect of the tissue-specific protein-peptide complex, obtained from *Sus scrofa* immune organs, on wound healing in *BALB/c* mice by percutaneous administration.

2. Materials and methods

2.1. Materials

Bioactive components, including proteins and peptides, were obtained as it was described earlier (Fedulova et al., 2017). Technology includes extraction of *Sus Scrofa*'s thymus, spleen and lymph nodes by water-salt solution (0.9% NaCl), with containing 50 ppm deuterium, then extracts were purified and frozen at -40 °C. Molecular composition was characterized in details earlier, in our previous article (Fedulova et al., 2018).

Lecithin liquid crystals (LLC) were prepared as it was described earlier (Murashova et al., 2019): 7.0 g of "Moslecithin" phospholipid concentrate (Vitaprom, Russia, containing 97 wt% phospholipid complex 22 wt% of which is phosphatidylcholine (lecithin), and vegetable oils (Botanica, Russia: 1.0 g of *Persea gratissima* oil and 0.5 g of *Melaleuca alternifolia* essential oil). Then, 1.5 ml of distilled water or 1.5 ml of distilled water and 0.3 g of methyluracil, or 1.0 ml of distilled water and 0.5 ml of protein-peptide complex (5 wt% protein) was added to the sample. This stage of water solubilization was carried out detailed for 3.5 h in a closed flask at 40 °C, with constant mechanical stirring until obtaining a homogeneous system. The homogeneity of the system and the presence of the liquid crystal structure were assessed by polarizing microscopy in transmitting light using an Axiostar Plus microscope (Zeiss, Germany). The results of polarizing microscopy showed that the samples had a texture typical for lamellar liquid crystals. Viscosity of liquid crystals of such composition was hundreds and tens of Pa·s at shear rates of 0.1–1.0 s⁻¹ (Murashova et al., 2019).

Liquid microemulsions (LME) were prepared as it was described earlier (Murashova et al., 2019): 2.0 g of Moslecithin phosphate lipid concentrate was dissolved in a mixture of 3.42 g of Vaseline oil and 3.43 g of *Persea gratissima* oil (Botanica, Russia) at 60 °C in a closed flask with constant stirring in a magnetic stirrer, RCT

basic (IKA, Germany) at 200 rpm for 80 min, until complete dissolution of the phospholipid concentrate. Then, 0.7 g of oleic acid and 0.45 g of *Melaleuca alternifolia* essential oil (Botanica, Russia) were added to the solution that had been cooled to 20 °C, which was then mixed at 100 rpm at 25 °C. Then, 7 ml of distilled water containing 5 wt% protein-peptide complex was injected into the obtained oil solution using a pipette-dispenser. Water solubilization was carried out under the action of ultrasound with a frequency 22 kHz and power 26.2 W for 1 min, and the sample was cooled to room temperature. The ultrasonification was repeated 3–4 times until complete solubilization of water phase. Obtained sample of the microemulsion was cooled to 20 °C. The absence of solid microparticles in the sample, liquid microdroplets and particles of the liquid crystalline phase was assessed using an Axiostar Plus polarization microscope with crossed and non-crossed polaroids. Average hydrodynamic diameter of microemulsion droplets was determined by dynamic light scattering method by Zetasizer Nano ZS (Malvern, UK) equipped with a He-Ne laser operating at 532 nm at temperature 25 °C. Hydrodynamic diameter of the droplets for the sample, containing water, was 21 ± 3 nm and for the sample, containing protein extract, was 44 ± 2 nm. Viscosity of microemulsions of such composition was in the range 1.0–0.1 Pa·s at shear rates of 1–10 s⁻¹ (Murashova et al., 2019).

2.2. Animal model

The research was performed on male mature clinically healthy sexually naive *BALB/c* specific-pathogen-free mice ($n = 68$), obtained from the Shemyakin-Ovchinnikov Institute of Bioorganic Chemistry RAS (Nursery for Laboratory Animals). Mice were adapted for 5 days to the conditions of individually ventilated cells in the Ehret system (Ehret, Germany), which creates an optimal microclimate equal in each individual cell: temperature 22 ± 3 °C, humidity 50–60%, light cycle 12 h light / 12 h dark. Throughout the experiment, the diet of mice (*ad libitum*) consisted of a complete feed compound (Laboratorykorm, Russia).

Animals were euthanized using carbon dioxide in a VetTech installation (VetTech Solutions Ltd., UK), in accordance with Directive 2010/63/EU of the European Parliament and the European Union Council for Protection of Animals used for scientific purposes. The mice were kept and exposed to all manipulations in compliance with European Community Directives 86/609EEC. The research was approved by the bioethical commission of the V.M. Gorbатов Federal Research Center for Food Systems of the Russian Academy of Sciences (protocol #02/2018, dated November 09, 2018).

2.3. Percutaneous administration of protein-peptide complex

Linear wound model was selected as most suitable to damage all layers of the epidermis and to get information about wound reduction on extract applied mice in compare to controls. The linear wound model was created as follows: under anesthesia by intramuscular Xyla (Interchemie Werken De Adelaar Eesti AS, Estonia) at 5 mg/kg and Zoletil 100 (Valdepharm, France) at 20 mg/kg, the fur and underfur were shaven off from the middle of the back, and longitudinal incision of the skin and subcutaneous fatty tissue (20 ± 1 mm in length) was made along the midline of the back. After the incision was cut, the wound edges were brought together using two equidistant silk sutures. Animals that received drugs percutaneously were exposed to the test drug starting on the day of the incision, and the test drug was applied to the wound surface daily for 8 days (Mayorova et al., 2018). All samples were removed before applying a new dose of ointment using a gauze swab moistened with distilled water.

The experiment was completed on the 9th day. After euthanasia using carbon dioxide in a VetTech installation (VetTech Solutions

Ltd., UK), in accordance with Directive 2010/63/EU of the European Parliament and the European Union Council for Protection of Animals used for scientific purposes., wound tensiometric parameters were evaluated for each animal (besides M group mice) by cutting a piece of the skin to obtain the wound surface (including 1.5 cm on either side of the scar). Using modified pharmacy weights, scar strength was then measured by suspending the load weight on the flap, scars were located in horizontal position. The initial weight was 100 g, and the load increment was 5 g in 30 s. The weight that caused the scar to break is referred to as the plummet weight.

M group consisted of healthy intact mice ($n = 11$). The reference group (W group) consisted of mice with the wound model ($n = 9$) that did not receive any treatment. To test the efficacy of percutaneous treatment using lecithin liquid crystals (LLC), mice were divided into 3 groups: (A) mice with the wound model, treated with 0.5 cm³ methyluracil ointment ($n = 10$); (B) mice with the wound model, treated using lecithin liquid crystals ($n = 9$); and (C) mice with the wound model, treated using lecithin liquid crystals containing the protein-peptide complex ($n = 10$). The mice that received drugs via percutaneous liquid microemulsion (LME) were divided into groups: (D) mice with a wound model, receiving treatment with an LME dummy ($n = 10$); (E) mice with a wound model, receiving the protein-peptide complex via LME ($n = 9$).

2.4. Histological studies

Histological studies were performed after scar strength measurement. Skin in count of 12 samples for each group were taken on both sides of wound edge (5×5 mm), next submerged in a neutral water solution of 10% formalin for 72 h at 22 ± 2 °C. Dehydration and paraffin soaking were performed in a Tissue-tek VIP 5 JR histological processor (Sakura, Japan). The skin samples were then embedded in paraffin blocks. Transverse sections 6 μ m thick were cut on a HM 325 rotary microtome (Microm International GmbH, Germany) and stained by hematoxylin and eosin (H&E), dehydrated, clarified and enclosed in a mounting medium CV Mount (Leica, UK). The histological preparations were observed using an Axio Imager A1 light microscope (magnification 40X), connected to an Axio Cam MRc 5 video camera, and images were processed on the Axio Vision 4.7.1.0 computer system (Carl Zeiss, Germany).

2.5. Haematological parameters

After experiment finished (on the 9th day) blood was taken from the hearts of the stunned animals into EDTA tubes (Aquisel, Spain). The blood was analyzed using the hematological analyzer Abacus Junior Vet 2.7 (Diatron Messtechnik GmbH, Austria), using reagent kits (Diatron). The following blood parameters were recorded: white blood cells count, red blood cells count, granulocytes, hemoglobin, hematocrit, platelet count and plateletcrit.

2.6. Statistical analysis

The results are presented as median and percentile values (P_{25} – P_{75}). The reliability of the differences in the average of the rank values between the groups was tested statistically using the nonparametric Kruskal – Wallis one-way analysis (for multiple independent groups), and the difference was considered significant at $p < 0.05$.

3. Results

Mice of all groups tolerated wound damage well. On the 2nd day after surgery, all mice showed an inflammatory phase of damage, primary tension and partial closure of the wounds, platelet

clot degradation occurred. In mice of W, A, and D groups redness, an increase in local temperature, and severe edema were noted. On the 4th day in all groups, the wound defects were filled with granulation tissue, which is probably associated with the migration of fibroblasts to the damaged area and the beginning of wound epithelization. Mice from group C showed completing wound closure on the 5th day, epithelization of wound in this group was faster minimum 2 days than in comparison W and B groups ($p < 0.05$), and it was approximately earlier 1 day compared to A group. In group E animals had total wound closure on the 6th day, that was faster 1 day compared to the W and D groups ($p < 0.05$). On the 7th day after damage, wound contraction and transformation of granulation tissue into scar tissue were also observed in W, B, and D groups, which were delayed compared to the C and E groups ($p < 0.05$). Moreover, protein-peptide complex via LLC and LME therapy resulted in significantly less scar formation (in its bulk) in mice compared to W group. It should be noted separately that in animals of C group on the 7th day after wound modeling, a more complete coat recovery was revealed.

Relative to the W group mice, scar tensiometric values (Fig. 1) were higher in B group by 53.8%, C group by 215.4%, D group by 76.9%, and E group by 161.5%, but there was no any difference between the mice from the A and reference groups ($p = 0.0916$). Relative to the mice, treated with methyluracil ointment, scar tensiometric values were higher in B group by 21.2%, C group by 148.5%, D group by 39.4%, and E group by 106.1%. Relative to the mice, treated using lecithin liquid crystals, tensiometric values

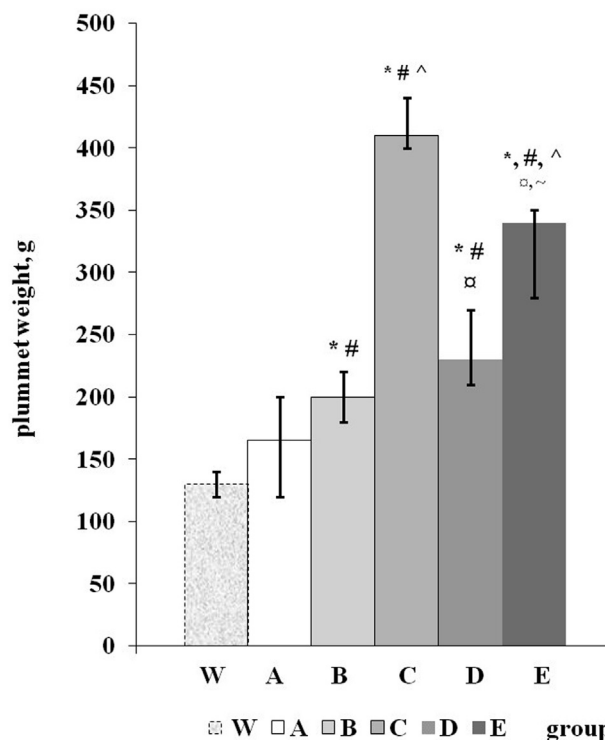


Fig. 1. Changes in scar tensiometric parameters of wounds treated percutaneously in mice. * is p -value < 0.05 compared to the group W; # is p -value < 0.05 compared to the group A; ^ is p -value < 0.05 compared to the group B; □ is p -value < 0.05 compared to the group C; ~ is p -value < 0.05 compared to the group D; group W is the reference group; A group consists of mice with the wound model, treated with 0.5 cm³ methyluracil ointment ($n = 10$); B group consists of mice with the wound model, treated using lecithin liquid crystals ($n = 9$); C group consists of mice with the wound model, treated using lecithin liquid crystals containing the protein-peptide complex ($n = 10$); D group consists of mice with a wound model, receiving treatment with an LME dummy ($n = 10$); E group consists of mice with a wound model, receiving the protein-peptide complex via LME ($n = 10$).

were higher in C group by 105.0% and E group by 70.0%, but there was no difference between B group and the group mice, receiving treatment with an LME dummy ($p = 0.0541$). Relative to the group C, the tensiometric parameters of the scar were respectively lower (Fig. 2) in D group and E group by 43.9% and 17.1%. And between D group mice and animals, receiving the protein-peptide complex via LME, took place difference by 32.4% ($p = 0.0025$) lower tensiometric value of the scar in D group (Fig. 1).

Histological examination of tissue sections of mice from group W showed an expansion of the connective tissue layer in the dermis, and increase numbers of macrophages and fibroblasts in the wounded area. Among the mice of groups A and D the scar retained

the dermal architectonics of collagen fibres, with elastic fibres thinned and fragmented in some places and compacted in others. The large number of fibres reflected the large number of fibroblasts. Analysis of tissue sections of mice from groups B, C and E, which all received percutaneous treatment, revealed maximal reepithelization and well-organized granulated connective tissue, consisting mainly of a layer of horizontally oriented fibres and fibroblasts; the epidermis is represented by multi-layered squamous keratinizing epithelium; in places where the hair comes to the surface of the skin the hair rods are braided with keratin layers; sebaceous glands form complexes with hair follicles. Cells of the dermis are localized mainly in the subepidermal areas. In tissue

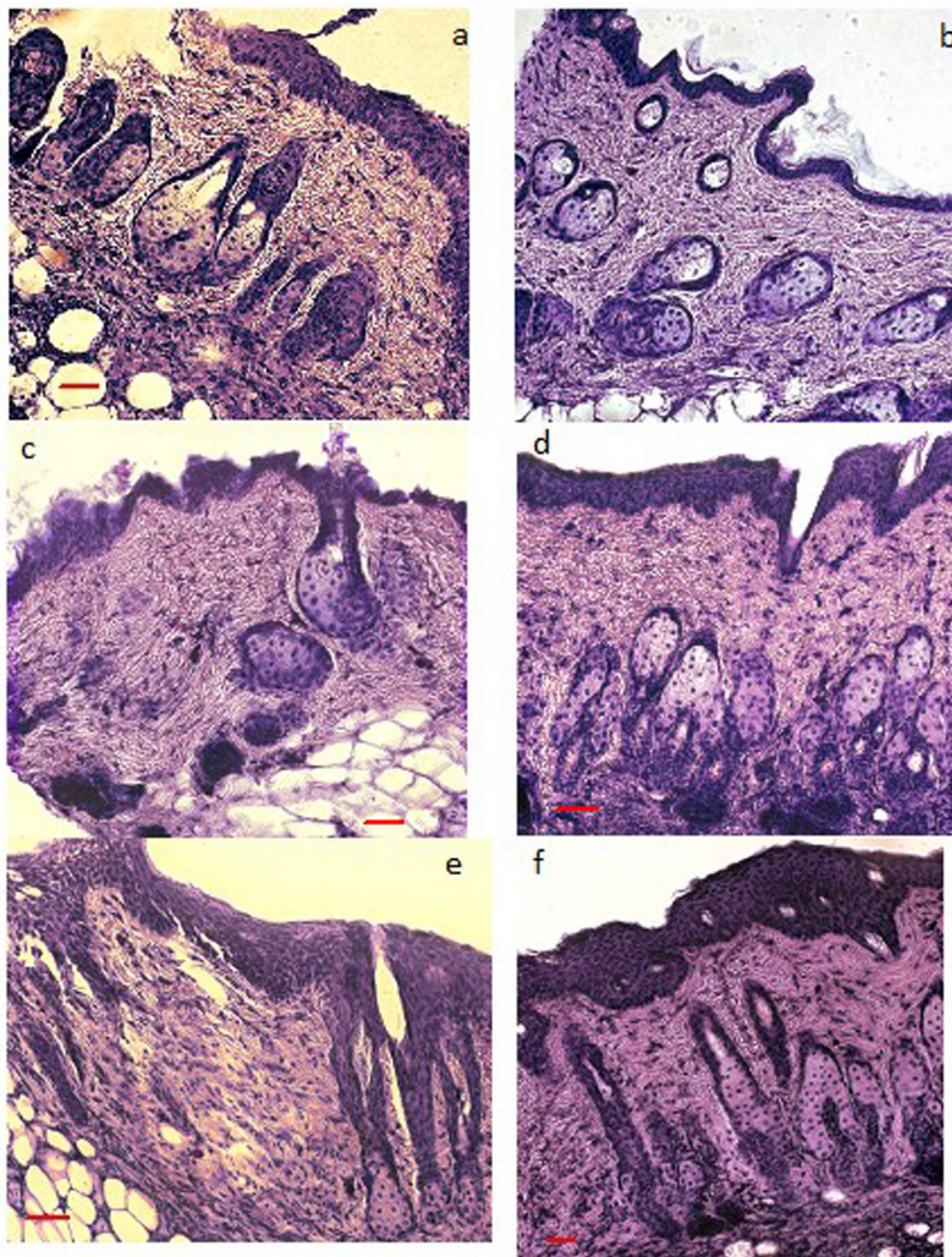


Fig. 2. H&E histology of scar tissue formation in treated wounds (a) Representative sections for each of the treatment groups. Red scale bar = 100 μm . Notes: a – group W; b – group A; c – group B; d – group C; e – group D; f – group E.

samples of group C mice, the vessels of the microvasculature and substratum capillaries network are highly visible (Fig. 2).

Albeit, relative to the intact healthy mice (M group), the W, A, B, and C groups had no difference of leukocyte and red blood cell counts ($p > 0.088$ and $p > 0.076$, respectively), nevertheless, in the animals in the last group were 38.7% and 32.4% lower lymphocytes and their relative proportion, 44.4% and 31.2% lower monocytes and their relative proportion, with 65.1% and 150.3% higher granulocytes and their relative proportion, 12.5% and 10.1% lower hemoglobin and hematocrit, respectively (Table 1). Whereas B group was different compared to M group not only monocytes and their relative count (by 44.4% and 37.5% lower, respectively), hemoglobin (by 13.1% lower) and hematocrit (by 7.4% lower), but also other indices: platelets by 27.3% and plateletcrit by 21.8% lower, respectively (Table 1). The most number of unequal indexes was in the A group in comparison to the intact animals: 13.0% lower relative lymphocytes, 13.0% and 65.1% higher granulocytes and their relative count, 33.3% and 56.2% lower monocytes and their relative count, 13.7%, 8.3%, 21.9%, and 20.0% lower hemoglobin, hematocrit, platelets, and plateletcrit, respectively (Table 1). The reference group without treatment was different compared to the M group 14.1% lower relative lymphocytes, 89.7% and 70.3% higher granulocytes and their relative proportion (respectively, Table 1), and 8.1% lower hematocrit.

Moreover, in contrast of the mice from A group, compared to the reference group mice the ones from C group had differences in leukocyte count (42.1% lower), lymphocytes and their relative count (47.0% and 21.2% lower, respectively), granulocyte relative count (46.9% higher), and, in addition, between C and W groups were not differences in monocyte relative count, platelets, and plateletcrits. In contrast of the B group, relative to the W group the mice from C group had the same changes in lymphocytes and their relative proportion (which was by 29.1% lower than in B group, $p < 0.001$), granulocyte relative percentage (which was in 1.96 times higher than in B group, $p < 0.001$), but they had nothing differences not only in platelets and plateletcrit, but also in granulocytes (which were in 2.21 times higher than in B group, $p = 0.022$). Also, relative to the W group, A group, B group, and C group mice

had decrease of monocyte counts (by 50.0% and more) and 12.1%, 11.5% and 10.9% lower hemoglobin levels (respectively, Table 1), but it was without any differences in the red blood cell counts ($p = 0.149$) and hematocrit ($p = 0.748$) in these groups relative to the reference group mice. Relative to the W group between A and B groups were differences in leukocyte count (23.9% lower in B group compared to the W), lymphocyte relative count (11.1% higher in B group compared to the W), granulocytes and their relative count (60.7% and 25.2% lower in B group compared to the W, respectively), relative monocytes (46.1% lower in A group compared to the W).

Relative to the intact M group, the reference group and groups of mice, receiving percutaneous liquid microemulsion, had no difference of leukocytes ($p = 0.175$), lymphocytes ($p = 0.874$), monocytes and their relative count ($p = 0.465$ and $p = 0.231$), red blood cell count ($p = 0.054$), platelets ($p = 0.297$), and plateletcrit ($p = 0.376$), nevertheless, the animals from group E had 18.0% lower lymphocyte relative percentage, 103.9% and 86.8% higher granulocytes and their relative proportion, 11.6% lower hematocrit, respectively (Table 2).

Although the mice from the W and D groups had the similar changes with the indexes of the E group, it was 10.1% lower hemoglobin in the D group relative to the M group. In addition, in contrast of the E group, the D group had the 10.8% lower relative lymphocyte count (which was also by 6.65% lower than in E group, $p = 0.010$), with 46.0% higher granulocytes, 8.48% lower hemoglobin, and 8.11% lower hematocrit relative to the average ranks of group W mice (Table 2). Relative to the reference group mice, the animals with a wound model, receiving the protein-peptide complex via LME showed also no differences in the other indexes, such as leukocytes and their relative proportions, red blood cell counts, platelets, and plateletcrit (p -values were from 0.145 to 0.859).

4. Discussion

The tissue- and species-specific protein-peptide complex included in lecithin liquid crystals and liquid microemulsion showed higher regeneration effect. It is well-known, that skin

Table 1
Blood results of mice received percutaneous lecithin liquid crystals.

Parameters (median, [P ₂₅ -P ₇₅])	Group M	Group W	Group A	Group B	Group C
LEU, 10 ⁹ /l	6.31 [3.96–8.56]	8.01 [6.70–10.31]	6.81 [5.88–9.77]	6.09 # [4.63–6.59]	4.63 # [4.08–6.59]
LYM, 10 ⁹ /l	4.76 [3.35–7.09]	5.51 [4.68–7.53]	4.70 [4.17–6.99]	4.49 [4.02–5.12]	2.92 *, □ [2.86–2.98]
Relative LYM, %	80.6 [74.8–84.7]	69.2 * [66.4–72.2]	70.1 * [67.5–77.0]	76.9 # [74.3–84.1]	54.5 ^, # [44.0–64.9]
GRAN, 10 ⁹ /l	1.26 [0.86–1.35]	2.39 ^ [2.02–3.03]	1.94 * [1.28–2.61]	0.94 □ [0.63–1.78]	2.08 ^ [1.39–3.65]
Relative GRAN, %	17.5 [14.0–23.5]	29.8 * [27.0–31.7]	28.9 * [22.3–31.8]	22.3 # [14.9–25.6]	43.8 ^, □ [33.7–55.4]
MON, 10 ⁹ /l	0.09 [0.06–0.14]	0.12 [0.09–0.13]	0.06 *, # [0.02–0.10]	0.05 *, □ [0.03–0.05]	0.05 *, # [0.03–0.07]
Relative MON, %	1.6 [1.3–1.8]	1.3 [1.1–1.4]	0.7 ^, # [0.5–1.0]	1.0 ^ [0.6–1.1]	1.1 * [0.6–1.4]
RBC, 10 ¹² /l	10.39 [9.96–11.16]	10.03 [9.86–10.14]	10.08 [9.93–10.34]	10.54 [10.02–10.78]	9.8 [9.6–10.2]
HGB, g/l	168 [162–182]	165 [158–166]	145 ^, # [144–146]	146 ^, # [144–149]	147 ^, # [136–154]
HCT, %	48.3 [46.5–50.8]	44.4 ^ [43.7–44.6]	44.3 ^ [43.4–44.8]	44.7 ^ [42.7–45.9]	43.4 ^ [42.6–44.8]
PLT, 10 ⁹ /l	916 [864–1038]	1016 [982–1063]	715 ^, □ [664–803]	667 ^, □ [632–703]	905 [739–950]
PCT, %	0.55 [0.52–0.64]	0.60 [0.56–0.64]	0.44 ^, □ [0.40–0.49]	0.43 ^, □ [0.39–0.43]	0.54 [0.46–0.58]

Note: * is p -value < 0.05 compared to the group M; ^ is p -value < 0.01 compared to the group M; # is p -value < 0.05 compared to the group W; □ is p -value < 0.01 compared to the group W; LEU: leukocytes; LYM: lymphocytes; GRAN: granulocytes; MON: monocytes; RBC: red blood cells; HGB: haemoglobin; HCT: haematocrit; PLT: platelets; PCT: plateletcrit.

Table 2
Blood results of mice received percutaneous liquid microemulsion.

Parameters (median, [P ₂₅ –P ₇₅])	Group M	Group W	Group D	Group E
LEU, 10 ⁹ /l	6.31 [3.96–8.56]	8.01 [6.70–10.31]	8.69 [6.12–10.04]	7.54 [6.50–10.23]
LYM, 10 ⁹ /l	4.76 [3.35–7.09]	5.51 [4.68–7.53]	4.76 [3.76–6.48]	4.98 [3.86–5.51]
Relative LYM, %	80.6 [74.8–84.7]	69.2 * [66.4–72.2]	61.7 ^, # [54.2–64.3]	66.1 * [63.0–67.6]
GRAN, 10 ⁹ /l	1.26 [0.86–1.35]	2.39 ^ [2.02–3.03]	3.49 ^, # [3.16–4.20]	2.57 ^ [2.22–3.64]
Relative GRAN, %	17.5 [14.0–23.5]	29.8 * [27.0–31.7]	36.4 ^ [34.1–43.2]	32.7 ^ [31.1–36.1]
MON, 10 ⁹ /l	0.09 [0.06–0.14]	0.12 [0.09–0.13]	0.15 [0.09–0.19]	0.07 [0.06–0.12]
Relative MON, %	1.6 [1.3–1.8]	1.3 [1.1–1.4]	1.5 [1.2–2.0]	1.1 [0.9–1.3]
RBC, 10 ¹² /l	10.39 [9.96–11.16]	10.03 [9.86–10.14]	9.61 [9.33–10.17]	9.78 [9.66–9.95]
HGB, g/l	168 [162–182]	165 [158–166]	151 *, # [142–153]	157 [151–162]
HCT, %	48.3 [46.5–50.8]	44.4 ^ [43.7–44.6]	40.8 ^, # [39.7–41.5]	42.7 ^ [41.6–44.3]
PLT, 10 ⁹ /l	916 [864–1038]	1016 [982–1063]	1064 [853–1202]	944 [910–1030]
PCT, %	0.55 [0.52–0.64]	0.60 [0.56–0.64]	0.64 [0.50–0.70]	0.54 [0.52–0.62]

Note: * is p-value < 0.05 compared to the group M; ^ is p-value < 0.01 compared to the group M; # is p-value < 0.05 compared to the group W; LEU: leukocytes; LYM: lymphocytes; GRAN: granulocytes; MON: monocytes; RBC: red blood cells; HGB: haemoglobin; HCT: haematocrit; PLT: platelets; PCT: plateletcrit.

wound healing consists of the overlapping stages: hemostasis, inflammation, proliferation and remodeling (Jee et al., 2016), which end with the scar formation. So expectedly, healing effect was relied on the ability of protein-peptide complex to promote the proliferation of skin layers which shortened the duration of some stages and accelerated the wound closure. Although on the 2^d day after wound modelling in mice of all groups there were observed inflammatory phase of wound healing, but in mice of W, A, and D groups the significant redness, increase in local temperature, and severe edema were noted and caused by the treatment without immune active species-specific proteins and peptides. In this period, more positive condition of the wounds in animals of C and E groups can be due to the properties of α -thymosin to influence on healing process as adjuvant for immune enhancement, which caused by inducing maturation, differentiation and function of immune effector cells (Goldstein, 2009), and also by reducing vicious inflammatory circle according to decreasing in pro-inflammatory cytokines (Malinda et al., 1998; Romani et al., 2006). Some of these effects achieves through ability of α -thymosin reacts with Toll-like receptors (TLR), such as TLR2 and TLR9, in myeloid and plasmacytoid dendritic cells, that leads to the proliferation of both dendritic and T-cells (Romani et al., 2004), and also arising of cytokine productions, primarily interleukin-2 and interferon-gamma (Wang et al., 2018). In addition, α -thymosin increases stem cell expansion (Tuthill and King, 2013), which can promote regeneration of the altered tissues. Besides this, cathepsin S C-fragment (CTSS), included in the new protein-peptide complex, functions in neutrophil degranulation, inflammatory processes, and responses to infection (Wilkinson et al., 2015), arising efficacy of the treatment. Similarly, protein myeloid differentiation primary response protein (MyD88), revealed us in complex by using two-dimensional gel electrophoresis (Fedulova et al., 2018), in plays an essential role in the transmission of signals involved in innate immunity, and is particularly involved in the cytokine neutrophil response, and in regulating activity of macrophages, dendritic and epithelial skin cells, and mucous membranes (Cervantes, 2017; Chernukha et al., 2017).

On the 4th day after modelling in mice of all groups it was started proliferation phase, but more effective filling wounds with granulation tissue were observed in E and, especially, C groups, which is probably associated with the migration of fibroblasts to the damaged area and the beginning of wound epithelization. More significant granulation tissue growth in mice of E and C groups allows earlier ingrowth of blood vessels that provide oxygen and nutrition to the growing tissue in optimal concentration, and also support more affective leukocyte migration to the wound site (Xue and Jackson, 2015). All of these phenomena can be provoked by the local administration of protein-peptide complex as results from its constituents, including their abilities to stimulate cell energy metabolism, accelerate synthesis of mitochondrial proteins and extracellular matrix (Garac, 2018), arise of DNA repairing and its transcription, increase rate of angiogenesis, and some others detailed presented below. The active constituents of new protein-peptide complex include transgelin (TAGLN) (Daniel et al., 2012), involved in epithelial cell differentiation; ubiquitin-carboxyl-terminal hydrolase isozyme L3, which regulates DNA repair, cell proliferation, development and differentiation, and responses to pathogens and stress (Liao et al., 2018; Wang et al., 2016); the homologue of the mitochondrial protein ES1, a factor contributing to the formation of megamitochondria, by increasing mitochondrial volume during hypertrophy and inflammation (Masuda et al., 2016); and GTP-binding nuclear protein RAN with N-terminal acetylation, which increases the activity of guanosine triphosphate and participates in cell division, organization of the mitotic spindle, regulation of protein binding, and DNA transcription (Zaoui et al., 2019).

At first, on the 5th day the epithelial regeneration had been finished completely in mice of C group, which had also enhanced collagen synthesis revealed due to the histological study. It is well-known, that contraction of wound is a necessary stage to optimize its healing (Pereira and Bártolo, 2014), and it requires replacing of collagen III type, produced throughout the proliferative phase, on stronger type I collagen. But higher production of collagen III type after long inflammatory phase of dermal healing frequently leads to the abnormal cutaneous scarring, such as hypertrophic or keloid

scars. Consequently (Lei et al., 2019), scar bulk decreasing in animals of the C group approves that inhibiting effect for scar formation takes place in them due to the less duration of the inflammation phase and accelerating wound healing via using lecithin liquid crystals containing the protein-peptide complex. Despite less scar bulk, their scar tensiometric value was the highest between all mice groups, that highlighted tremendous potential for using of the new complex in dermal wound healing. The epithelial regeneration in animals of E group was later (in 1 day, than in C group), which had transformation of granulation tissue to scar tissue with contraction of the wound on the 6th day; but it was faster compared to the W and D groups. In addition, mice of E group had higher scar tensiometric value in comparison other groups, excluding C one, which on the 7th day after wound modeling had also more complete coat recovery, than other groups. So, LME exerted comparable scar healing capacity in comparison to LLC. However, LLC resulted in greater cell proliferation and better granulation tissue formation and epithelialization. This difference could be due to the higher viscosity of LLC, and consequently slower diffusion, thus causing a more prolonged effect of the applied substances. The above-mentioned proteins may also trigger a cascade of reactions within the proliferative nodes of the hair follicles, via the transfollicular pathway, thus activating dormant stem cells, which, in their turn, become progenitor cells; these then promote more efficient epidermal stratification accompanied by less local and systemic disruption of homeostasis.

Wound healing occurred faster in mice that received the protein-peptide complex via LLC and LME, because of resorption through the skin of bioactive high molecular-weight compounds by transpapendegal routes, via sebaceous, sweat glands and hair follicles (Alkilani et al., 2015); further, the low molecular-weight compounds were able to penetrate by diffusion through epidermal cells or cellular junctions (pores) (Abu Hashim et al., 2018; Andrews et al., 2013). Wound healing occurs faster when tissue dehydration and subsequent cell death were prevented by the maintenance of the liquid phase (Bykov et al., 2017; Driver, 2016; Ludolph et al., 2018). Besides, during the liquid phase there is longer exposure to bioactive substances; they are dissolved and transported better than under dry conditions. The liquid phase facilitates removal of necrotic tissue and fibrin, and helps to form an additional protective barrier (Gonzalez et al., 2016). In the study the latest was confirmed by higher scar tensiometric parameters and better hystological data in mice of B and D groups in comparison to the W and A groups (Fig. 1, Fig. 2).

The liquid phase of wound healing stimulates epithelial development and accelerates tissue granulation. Also, the promoting of tissue remodeling can be due to a decrease in lymphocytes recruitment during granulocytes production stimulation and antifibrotic polarization of macrophages into which blood monocytes are transformed (Larouche et al., 2018; Mu et al., 2014). Low molecular-weight peptides of the new complex can penetrate partially by diffusion through epidermal cells or intercellular junctions; these, together with inner high molecular-weight proteins, have, probably, an additive and synergistic effect on immune system along, further modifying the activity of immunocompetent cells. The data of hematological analysis also showed that there were only some effects in blood using new protein-peptide complex both it combinations with lecithin liquid crystals and liquid microemulsion, mostly in leukocytes, such as white blood cell count, lymphocytes, granulocytes, monocytes, and their relative counts (Table 1). And these changes were more often in animals of the C group compared to the E group (Table 2), that allowed to differentiate significances of LLC and LME systemic influences. A decrease in the level of lymphocytes in group C animals may be due to their release from the circulation for the implementation of regulatory protective functions directly in the endothelial tis-

sues, as well as, possibly, in the underlying connective tissue and peripheral immune organs. In particular, it is known that up to 15% of circulating blood cells are CLA-positive T-lymphocytes associated with the cutaneous lymphocyte antigen CLA, which is considered a receptor that controls the affinity of T-lymphocytes for the skin (Ni and Walcheck, 2009; De Jesús-Gil et al., 2018). It can be assumed that the investigated biomolecules, on the one hand, send CLA-positive T-lymphocytes from the bloodstream to the inflammation focus, and on the other hand, increase the functional activity of lymphocytes and other leukocytes remaining in the blood. A decrease in the level of hemoglobin in the blood of experimental animals may be due to its binding by macrophages of the tissue reticuloendothelial system to accelerate the processes of wound healing (Avishai et al., 2017; Krzyszczyk et al., 2018). The influence of the complex on the blood cells can be caused mainly by the α -thymosin (C3VVV8_PIG, m/z 3802.8), which induces the proliferation and differentiation of lymphocytes, activates the phagocytic function of granulocytes, and also leads to elevating of the lymphocyte and granulocyte counts. The statement of their larger impacting on leukocytes was confirmed by the absence of the any changes in the red blood cell counts, haemoglobins, haematocrits, platelet counts, and plateletcrits between B group and C group mice (both were receiving lecithin liquid crystals, Table 1), and between D group and E group mice (both were receiving liquid microemulsion, (Table 2), which had differences only in the using new protein-peptide complex. So, all of these pointed out on predominant of the local effect of the complex, extracted from *Sus scrofa* immune organs.

So, all of above-mentioned obviously pointed out on predominant of the local effect of the LLC and LME with new complex, extracted from *Sus scrofa* immune organs.

5. Conclusions

Thus, the accelerating dermal wound healing, which is essential for better health of affected animals, can be achieved by using of bioactive substances, obtained from *Sus Scrofa* immune tissues. This work sought to investigate a practical potential for bioactive product obtained us in previous studies. Our findings indicate that percutaneous (local) administration of the protein-peptide complex vigorously activates wound healing in the animals, probably, via the action of the tissue- and species-specific protein-peptide complexes.

It is possible may be caused by particular changes in the skin when the complex is applied to the wound surface; these include changes such as the fragmentation caused by S-terminus cathepsin S (STSS), and those caused by α -thymosin *Sus scrofa* (C3VVV8_PIG, m/z 3802.8), the protein myeloid differentiation primary response protein (MyD88), transgelin (TAGLN), isoform XI ubiquitin carboxyl-terminal hydrolase isozyme L3, homologue mitochondrial protein ES1, and the isoform 1 of the GTP-binding nuclear protein RANcN-terminal acetylation. This active pattern alters not only the local immunological reactivity of the skin, but also, stimulates neovascularization, enhances the growth of granulation tissue and activates stem cells in the hair follicles, further promoting the healing processes at the wound surface. The preliminary protective effect of the new bioactive complex on development abnormal cutaneous scarring was also demonstrated due to the decreasing scar bulk more significant in mice receiving the protein-peptide complex via LME and, especially, LLC. It is worth being noted, that the scar tensiometric values of the same groups were respectively higher by 161.5% and 215.4% relative to the animals, which did not receive tissue-specific substances for promoting of skin wound healing. Also, it should be indicated to the predominant of the local effect of the LLC and LME with new complex, whereas its influences were little on the leukocytes in blood and insignificant on the red blood cell count and hemoglobin level.

Administration of the protein-peptide complex via LLC showed improved better bioavailability and stimulated the wound healing more than administration via LME. This is a result of the higher viscosity of LLC, which may therefore have a prolonged effect, both due to the slow release of molecular protein factors, and through the direct creation of a liquid phase that prevents skin dehydration and cell death, thereby contributing to faster wound healing.

So, protein-peptide complex, obtained from *Sus scrofa* immune organs, can be not only potential biomaterial for promoting of wound regeneration, but also may be contemplated as basis for development new effective wound-healing agent in combination with lecithin liquid crystals.

Funding

This work was supported by the Russian Science Foundation (RSF) grant number 19-76-10034.

Declaration of Competing Interest

The authors declare that they have no known competing financial interests or personal relationships that could have appeared to influence the work reported in this paper.

References

- Abdulbaqi, I.M., Darwis, Y., Khan, N.A., Assi, R.A., Khan, A.A., 2016. Ethosomal nanocarriers: the impact of constituents and formulation techniques on ethosomal properties, in vivo studies, and clinical trials. *Int. J. Nanomed.* 25 (11), 2279–2304. <https://doi.org/10.2147/IJN.S105016>.
- Abu Hashim, I.I., Abo El-Magd, N.F., El-Sheakh, A.R., Hamed, M.F., Abd El-Gawad, A.E. H., 2018. Pivotal role of Acitretin nanovesicular gel for effective treatment of psoriasis: ex vivo-in vivo evaluation study. *Int. J. Nanomed.* 13, 1059–1079. <https://doi.org/10.2147/IJN.S156412>.
- Alkilani, A.Z., McCrudden, M.T., Donnelly, R.F., 2015. Transdermal drug delivery: innovative pharmaceutical developments based on disruption of the barrier properties of the stratum corneum. *Pharmaceutics* 7 (4), 438–470. <https://doi.org/10.3390/pharmaceutics7040438>.
- Andrews, S.N., Jeong, E., Prausnitz, M.R., 2013. Transdermal delivery of molecules is limited by full epidermis, not just stratum corneum. *Pharm. Res.* 30 (4), 1099–1109. <https://doi.org/10.1007/s11095-012-0946-7>.
- Avishai, E., Yeghiazaryan, K., Golubnitschaja, O., 2017. Impaired wound healing: facts and hypotheses for multi-professional considerations in predictive, preventive and personalised medicine. *EPMA J.* 8, 23–33. <https://doi.org/10.1007/s13167-017-0081-y>.
- Baradaran, M., Jalali, A., Soorki, M.N., Galehdari, H., 2017. A novel defensin-like peptide associated with two other new cationic antimicrobial peptides in transcriptome of the Iranian Scorpion Venom. *Iran. Biomed. J.* 21 (3), 190–196. <https://doi.org/10.18869/acadpub.ijb.21.3.190>.
- Basov, A.A., Fedulova, L.V., Baryshev, M.G., Dzhimak, S.S., 2019. Deuterium-depleted water influence on the isotope $^2\text{H}/^1\text{H}$ regulation in body and individual adaptation. *Nutrients* 11, 1903. <https://doi.org/10.3390/nu11081903>.
- Bykov, I.M., Basov, A.A., Malyshko, V.V., Dzhimak, S.S., Fedosov, S.R., Moiseev, A.V., 2017. Dynamics of the pro-oxidant/antioxidant system parameters in wound discharge and plasma in experimental purulent wound during its technological liquid phase treatment. *Bull. Exp. Biol. Med.* 163 (2), 268–271. <https://doi.org/10.1007/s10517-017-3781-3>.
- Cervantes, J.L., 2017. MyD88 in Mycobacterium tuberculosis infection. *Med. Microbiol. Immunol.* 206 (3), 187–193. <https://doi.org/10.1007/s00430-017-0495-0>.
- Chaulagain, B., Jain, A., Tiwari, A., Verma, A., Jain, S.K., 2018. Passive delivery of protein drugs through transdermal route. *Artif. Cells Nonomed. Biotechnol.* 19, 1–16. <https://doi.org/10.1080/21691401.2018.1430695>.
- Chen, D., Liu, H., Wang, Y., Chen, S., Liu, J., Li, W., Dou, H., Hou, W., Meng, M., 2019. Study of the adoptive immunotherapy on rheumatoid arthritis with thymus-derived invariant natural killer T cells. *Int. Immunopharmacol.* 67, 427–440. <https://doi.org/10.1016/j.intimp.2018.12.040>.
- Chernukha, I.M., Fedulova, L.V., Kotenkova, E.A., Takeda, S., Sakata, R., 2018. Hypolipidemic and anti-inflammatory effects of aorta and heart tissues of cattle and pigs in the atherosclerosis rat model. *Animal Sci. J.* 89 (5), 784–793. <https://doi.org/10.1111/asj.12986>.
- Chernukha, I.M., Fedulova, L.V., Vasilevskaya, E.R., Kotenkova, E.A., 2017. Comparative study of biocorrective protein-peptide agent to improve quality and safety of livestock products. *Potravinarstvo Slovak J. Food Sci.* 11 (1), 539–543. <https://doi.org/10.5219/590>.
- Crosby, C.M., Kronenberg, M., 2018. Tissue-specific functions of invariant natural killer T cells. *Nat. Rev. Immunol.* 18 (9), 559–574. <https://doi.org/10.1038/s41577-018-0034-2>.
- Daniel, C., Lüdke, A., Wagner, A., Todorov, V.T., Hohenstein, B., Hugo, C., 2012. Transgelin is a marker of repopulating mesangial cells after injury and promotes their proliferation and migration. *Lab. Invest.* 92 (6), 812–826. <https://doi.org/10.1038/labinvest.2012.63>.
- De Jesús-Gil, C., Ruiz-Romeu, E., Ferran, M., Chiriach, A., Deza, G., Hólló, P., Celada, A., Pujol, R.M., Santamaria-Babi, L.F., 2018. CLA+ T cell response to microbes in psoriasis. *Front. Immunol.* 9, 1488. <https://doi.org/10.3389/fimmu.2018.01488>.
- Driver, R.K., 2016. Utilizing the VeraFlo™ instillation negative pressure wound therapy system with advanced care for a case study. *Cureus* 8 (11), e903. <https://doi.org/10.7759/cureus.903>.
- Fedulova, L.V., Basov, A.A., Vasilevskaya, E.R., Dzhimak, S.S., 2019. Gender difference response of male and female immunodeficiency rats treated with tissue-specific biomolecules. *Curr. Pharm. Biotechnol.* 20 (3), 245–253. <https://doi.org/10.2174/1389201020666190222184814>.
- Fedulova, L., Elkina, A., Vasilevskaya, E., Barysheva, E., 2018. Identification of tissue-specific proteins of immunocompetent organs of *Sus scrofa* isolated in deuterium depleted medium. *Med. Sci.* 22 (9), 509–513.
- Fedulova, L.V., Vasilevskaya, E.R., Kotenkova, E.A., Elkina, A.A., Baryshev, M.G., Lisitsyn, A.B., 2017. Influence of different polypeptides fractions derived from *Sus Scrofa* immune organs on the rats immunological reactivity. *J. Pharm. Nutr. Sci.* 7 (2), 35–40. <https://doi.org/10.6000/1927-5951.2017.07.02.1>.
- Garac, E., 2018. From thymus to cystic fibrosis: the amazing life of thymosin alpha 1. *Expert Opin. Biol. Ther.* 18 (1), 9–11. <https://doi.org/10.1080/14712598.2018.1484447>.
- Goldstein, A.L., 2009. From lab to bedside: Emerging clinical applications of thymosin α 1. *Expert Opin. Biol. Ther.* 9, 593–608. <https://doi.org/10.1517/14712590902911412>.
- Gonzalez, A.C., Costa, T.G., Andrade, Z.A., Medrado, A.R.A.P., 2016. Wound healing – a literature review. *An Bras Dermatol.* 91 (5), 614–620. <https://doi.org/10.1590/abd1806-4841.20164741>.
- Grebennikova, S.V., Maklyakov, Y.S., 2018. Experimental and clinical study of the efficacy of medicines containing omega-3 and 6 polyunsaturated fatty acids, in the treatment of inflammatory skin diseases. *Res. Res. Pharmacol.* 4 (2), 85–93. <https://doi.org/10.3897/rpharmacology.4.28420>.
- Gudyrev, O., Andronova, T., Nesterova, E., 2018. The results of the study of the carcinogenic properties of glucosaminylmuramyl dipeptide GMDP in chronic experiments in mice and rats. *Res. Res. Pharmacol.* 4 (4), 97–106. <https://doi.org/10.3897/rpharmacology.4.32191>.
- Jee, C.H., Eom, N.Y., Jang, H.M., Jung, H.W., Choi, E.S., Won, J.H., Hong, I.H., Kang, B.T., Jeong, D.W., Jung, D.I., 2016. Effect of autologous platelet-rich plasma application on cutaneous wound healing in dogs. *J. Vet. Sci.* 17, 79–87. <https://doi.org/10.4142/jvs.2016.17.1.79>.
- Kalkhof, S., Förster, Y., Schmidt, J., Schulz, M.C., Baumann, S., Weißflog, A., Gao, W., Hempel, U., Eckelt, U., Rammelt, S., Von Bergen, M., 2014. Proteomics and Metabolomics for In Situ Monitoring of Wound Healing. *Biomed. Res. Int.* 2014, e934848. <https://doi.org/10.1155/2014/934848>.
- Krzyszczczyk, P., Schloss, R., Palmer, A., Berthiaume, F., 2018. The role of macrophages in acute and chronic wound healing and interventions to promote pro-wound healing phenotypes. *Front. Physiol.* 9, 419. <https://doi.org/10.3389/fphys.2018.00419>.
- Larouche, J., Sheoran, S., Maruyama, R., Martino, M.M., 2018. Immune regulation of skin wound healing: mechanisms and novel therapeutic targets. *Adv. Wound Care (New Rochelle)* 7 (7), 209–231. <https://doi.org/10.1089/wound.2017.0761>.
- Lei, Z.Y., Chen, J.J., Cao, Z.J., Ao, M.Z., Yu, L.J., 2019. Efficacy of Aeschynomene indica L. leaves for wound healing and isolation of active constituent. *J. Ethnopharmacol.* 228, 156–163. <https://doi.org/10.1016/j.jep.2018.08.008>.
- Liao, C., Beveridge, R., Hudson, J.J.R., Parker, J.D., Chiang, S.C., Ray, S., Ashour, M.E., Sudbery, I., Dickman, M.J., El-Khamisy, S.F., 2018. UCHL3 regulates topoisomerase-induced chromosomal break repair by controlling TDP1 proteostasis. *Cell Rep.* 23 (11), 3352–3365. <https://doi.org/10.1016/j.celrep.2018.05.033>.
- Ludolph, I., Fried, F.W., Knepp, K., Arkudas, A., Schmitz, M., Horch, R.E., 2018. Negative pressure wound treatment with computer-controlled irrigation/instillation decreases bacterial load in contaminated wounds and facilitates wound closure. *Int. Wound J.* 15 (6), 978–984. <https://doi.org/10.1111/iwj.12958>.
- Malinda, K.M., Sidhu, G.S., Banaudha, K.K., Gaddipati, J.P., Maheshwari, R.K., Goldstein, A.L., Kleinman, H.K., 1998. Thymosin alpha 1 stimulates endothelial cell migration, angiogenesis, and wound healing. *J. Immunol.* 160, 1001–1006.
- Masuda, T., Wada, Y., Kawamura, S., 2016. ES1 is a mitochondrial enlarging factor contributing to form mega-mitochondria in zebrafish cones. *Sci. Rep.* 6, e22360. <https://doi.org/10.1038/srep22360>.
- Mayorova, A., Sysuev, B., Kchanaliyeva, I., Tretyakova, E., Evseeva, S., Sokolova-Merkuriyeva, A., 2018. Investigation of the bischofite gel reparative effect on the linear wound model. *Res. Res. Pharmacol.* 4 (3), 87–93. <https://doi.org/10.3897/rpharmacology.4.30697>.
- Mu, L., Tang, J., Liu, H., et al., 2014. A potential wound-healing-promoting peptide from salamander skin. *FASEB J.* 28 (9), 3919–3929. <https://doi.org/10.1096/fj.13-248476>.
- Murashova, N.M., Trofimova, E.S., Kostyuchenko, M.Y., Mezina, E.D., Yurtov, E.V., 2019. Microemulsions and lyotropic liquid crystals of lecithin as systems for transdermal drug delivery. *Nanotechnol. Russ.* 14 (1–2), 68–73. <https://doi.org/10.1134/S1995078019010075>.

- Ni, Z., Walcheck, B., 2009. Cutaneous lymphocyte-associated antigen (CLA) T cells up-regulate P-selectin ligand expression upon their activation. *Clin. Immunol.* 133 (2), 257–264. <https://doi.org/10.1016/j.clim.2009.07.010>.
- Novoseletskaya, A.V., Kiseleva, N.M., Belova, O.V., Zimina, I.V., Inozemtsev, A.N., Arion, V.Y., Sergienko, V.I., 2015a. The influence of the thymus peptides on analgesia caused by acute and chronic immobilization. *Vestn. Ross. Akad. Med. Nauk.* 1, 113–117. <https://doi.org/10.15690/vramn.v70i1.1240>.
- Novoseletskaya, A.V., Kiseleva, N.M., Zimina, I.V., Bystrova, O.V., Belova, O.V., Inozemtsev, A.N., Arion, V.Y., Sergienko, V.I., 2015b. Thymus polypeptide preparation tactivin restores learning and memory in thymectomized rats. *Bull. Exp. Biol. Med.* 159 (5), 623–625. <https://doi.org/10.1007/s10517-015-3030-6>.
- Pereira, R.F., Bártolo, P.J., 2014. Traditional therapies for skin wound healing. *Adv. Wound Care* 5, 208–229. <https://doi.org/10.1089/wound.2013.0506>.
- Romani, L. et al., 2004. Thymosin alpha 1 activates dendritic cells for antifungal Th1 resistance through toll-like receptor signaling. *Blood* 103, 4232–4239.
- Romani, L., Bistoni, F., Perruccio, K., et al., 2006. Thymosin alpha1 activates dendritic cell tryptophan catabolism and establishes a regulatory environment for balance of inflammation and tolerance. *Blood* 108 (7), 2265–2274.
- Tuthill, C.W., King, R.S., 2013. Thymosin alpha 1—A peptide immune modulator with a broad range of clinical applications. *Clin. Exp. Pharmacol.* 3 (4), e1000133. <https://doi.org/10.4172/2161-1459.1000133>.
- Tverskoi, A.V., Zhuchenko, M.A., Kolesnichenko, P.D., Morozova, E.N., Morozov, V.N., 2018. Effect of carbamylated darbepoetin administration at different doses on the thymus and spleen structure of rats. *J. Int. Pharmac. Res.* 45, 420–423.
- Vasilevskaya, E.R., Akhremko, A.G., 2019. Proteomic study of pig's spleen. *Potravinarstvo Slovak J. Food Sci.* 13 (1), 314–317. <https://doi.org/10.5219/1093>.
- Wang, M., Yu, T., Hu, L., Cheng, Z., Li, M., 2016. Ubiquitin carboxy-terminal HydrolaseL3 correlates with human sperm count, motility and fertilization. *PLoS One* 11 (10), e0165198. <https://doi.org/10.1371/journal.pone.0165198>.
- Wang, F., Yu, T., Zheng, H., et al., 2018. Thymosin alpha1-Fc modulates the immune system and down-regulates the progression of melanoma and breast cancer with a prolonged half-life. *Sci. Rep.* 8, e12351. <https://doi.org/10.1038/s41598-018-30956-y>.
- Wilkinson, R.D.A., Williams, R., Scott, C.J., Burden, R.E., 2015. Cathepsin S: therapeutic, diagnostic, and prognostic potential. *Biol. Chem.* 396 (8), 867–882. <https://doi.org/10.1515/hsz-2015-0114>.
- Xue, M., Jackson, C.J., 2015. Extracellular matrix reorganization during wound healing and its impact on abnormal scarring. *Adv. Wound Care (New Rochelle)* 4 (3), 119–136. <https://doi.org/10.1089/wound.2013.0485>.
- Yang, F., Qin, X., Zhang, T., Zhang, C., Lin, H., 2019. Effect of oral administration of active peptides of *pinctada martensii* on the repair of skin wounds. *Mar. Drugs* 17 (12), e697. <https://doi.org/10.3390/md17120697>.
- Zaoui, K., Boudhraa, Z., Khalifé, P., Carmona, E., Provencher, D., Mes-Masson, A.M., 2019. Ran promotes membrane targeting and stabilization of RhoA to orchestrate ovarian cancer cell invasion. *Nat. Commun.* 10 (1), e2666. <https://doi.org/10.1038/s41467-019-10570-w>.